

Impact of pH on molecular structure and surface properties of lentil legumin-like protein and its application as foam stabilizer

M. Jarpa-Parra^a, F. Bamdad^a, Z. Tian^a, Hongbo Zeng^b, Feral Temelli^a, L. Chen^{a,*}

^a Department of Agricultural, Food and Nutritional Science, University of Alberta, Canada

^b Department of Chemical and Materials Engineering, University of Alberta, Canada



ARTICLE INFO

Article history:

Received 24 February 2015

Received in revised form 29 April 2015

Accepted 30 April 2015

Available online 11 May 2015

Keywords:

Lentil protein

Foaming

Dilatational

Shear

Conformation

ABSTRACT

The capacity of a protein to form and stabilize foams and emulsions depends on its structural characteristics and its physicochemical properties. The structural properties of lentil legumin-like protein including molecular weight, hydrodynamic size, surface charge and hydrophobicity, and conformation were studied in relation to its air–water interfacial behaviors. Kinetics study suggested that the foaming stability was closely related to the surface conformation of the protein that strongly affected adsorption and reorganization of the protein layer at the air–water interface. Foams prepared at neutral pH showed dense and strong networks at the interface, where combination of the α -helix secondary structure, medium hydrodynamic molecular size, and balance between solubility/hydrophobicity all contributed to the formation of such strong protein network at the interface. At pH 5.0, the protein formed a dense and thick network composed of randomly aggregated protein particles at the air–water interface. Whereas at pH 3.0, the unordered structure increased intra-protein flexibility producing a less compact and relaxed interface that reduces elasticity modulus with time and reduced foam resistance against collapse. This research revealed that lentil legumin-like protein could form long-life foams at mild acidic and neutral pH. The potential for use of lentil protein as a novel foaming plant-based stabilizer is demonstrated in food and non-food applications where stable, long-life foams are required.

© 2015 Elsevier B.V. All rights reserved.

1. Introduction

Increasing cost of dairy-based ingredients, emerging dietary preferences (e.g., gluten-free and vegan) and consumer demand for healthier ingredients are leading the market trends toward lower cost and plant-based alternatives, which are gaining increasing market share as food ingredients and for bio-based material applications [1]. In this context, legume proteins are attracting attention because of potential from both nutrition and health standpoint. In general, legumes are high in protein (20–25%). The majority of storage proteins in legumes are globulins, which can be classified in two groups. Proteins in the first group have sedimentation coefficients between 10.5S and 13.0S and are referred to as ‘legumin-like’ or 11S proteins. The second group has smaller sedimentation coefficients (7.0–9.0S) and are generally isolated from seed extracts as trimers of glycosylated subunits. This group of proteins is referred to as ‘vicilin-like’ or 7S proteins [2]. Lentil is a leguminous plant high in fiber, low in fat and cholesterol free. Canada is one of the major lentil

producers in the world with an annual production of over 1.5 million tons [3]. Lentils contain 20.6–31.4% protein with legumin-like protein (~50%) as the major globulin fraction, which is comprised of a number of 6–19 polypeptides with a molecular weight (M_w) of 18–43 kDa [4]. Generally, it is accepted that legumin is a hexamer with a M_w of about 320–380 kDa, which consists of six polypeptide pairs that interact non-covalently. Each of these polypeptide pairs is comprised of an acidic subunit of about 40 kDa and a basic sub-unit of about 20 kDa, linked by a single disulfide bond [4]. Unlike other legumes such as soybean and pea, which have been extensively studied [5], there is limited research on the legumin-like protein of lentil except for some report on its sedimentation speed [6], immunological reactivity, composition [4], and functionalities, including foaming properties [7,8]. A fundamental understanding of detailed structural features of lentil legumin and its functionalities is important for its potential food applications.

In our previous work [9], extraction process parameters were optimized to obtain lentil protein concentrates, and they demonstrated strong foaming capacity and stability, comparable to whey and egg protein. This superior functionality may provide an opportunity for lentil protein to be used as a foaming agent of plant origin for both food and non-food applications. In spite of its high

* Corresponding author. Tel.: +1 780 492 0038; fax: +1 780 492 4265.

E-mail address: lingyun.chen@ualberta.ca (L. Chen).

potential, the underlying mechanism of such foaming properties of a plant protein is still unknown. As the major protein in lentil, legumin-like protein component could play an important role contributing to the foaming properties. Thus, this study aims to isolate and purify the legumin-like protein from lentil, and use it as a plant protein model to understand how protein molecular structure (molecular weight, surface charge, hydrophobicity, and conformation) impacts its surface properties (surface tension, dilatational and shear rheology), and subsequently foaming functionality. The generated knowledge may help develop strategies for modification of plant protein structures to improve their functionality for targeted applications. Most of the previous reports have focused on protein surface properties and foaming capacity at neutral pH. Our previous study revealed that environmental pH significantly influenced protein physicochemical properties and foaming functionality. Thus, the impact of environmental pH on the structure and properties of the lentil legumin-like protein was also investigated.

2. Materials and methods

2.1. Raw materials

Large green lentil produced in Saskatchewan, Canada of mixed varieties (Greenland and Sovereign) was purchased from a local supermarket (Superstore, Edmonton, AB, Canada). The grains were ground into fine flour using a Retsch centrifugal grinding mill with screen aperture size of 0.5 mm (ZM 200, Retsch, Inc., Newtown, PA, USA). The flour was packed in plastic bags, sealed, and stored at 4 °C until extraction. Standard protein molecule markers for SDS-PAGE (Precision Plus ProteinTM, M_w 10–250 kDa) and native electrophoresis (NativeMarkTM, M_w 20–1236 kDa) were purchased from Bio-Rad (Richmond, CA, USA) and Life Technologies (Burlington, ON, Canada), respectively. 1-Anilino-8-naphthalene-sulfonate (ANS) and the standard molecular markers for HPLC analysis (thyroglobulin, 670 kDa; ferritin, 440 kDa; BSA, 67 kDa; ovalbumin, 43 kDa; cytochrome C, 13.6 kDa and aprotinin, 6.5 kDa) were purchased from Sigma-Aldrich (St. Louis, MO, USA). All other chemicals were reagent grade.

2.2. Lentil legumin-like protein purification

Lentil protein concentrate (85 g of protein/100 g of concentrate) was obtained according to our previous study [9]. Legumin-like protein was purified from lentil protein concentrate by rate-zonal centrifugation using a sucrose lineal density gradient according to Abe and Davies [10]. Briefly, two sucrose solutions (12 and 60 g/100 mL) were kept overnight at 4 °C. Then, 13 mL of the 60 g/100 mL sucrose solution was placed into an OptisealTM centrifuge tube and 13 mL of the 12 g/100 mL sucrose solution was slowly layered at the top, so as not to disturb the previous one. Then, the centrifuge tubes were horizontally laid and kept at 4 °C overnight to produce the lineal sucrose gradient. The next day, the tubes were slowly returned to the vertical position and stored for 2 days at 4 °C. Meanwhile, a solution of 10 mg of protein concentrate/mL at pH 8 was stirred overnight at 4 °C. Then, 3 mL of the protein solution was placed on the top of the sucrose gradient and centrifuged at 302,000 × g for 4.5 h, using an OptimaXPN-80 ultracentrifuge (Beckman Coulter Canada LP, ON, Canada). Twelve fractions of approximately 2.4 mL each were immediately collected by puncture and elution from the bottom of each tube. The collected fractions were numbered from top to bottom and analyzed by native electrophoresis and SDS-PAGE. The sedimental velocity of the fraction was also calculated, based on rate-zonal centrifugation results. The fractions identified as legumin-like protein were

pooled and dialyzed for 96 h (Spectra/Por[®] 3 standard RCTubing, MWCO 3.5 kDa, Spectrum Laboratories, Inc.) and freeze dried. Then, all freeze dried fractions from different batches were pooled together to be tested. Purity of lentil legumin-like protein was measured using a nitrogen analyzer (FP-428, Leco Corporation, St. Joseph, MI, USA) giving a result of 81 g of protein/100 g of isolate.

2.3. Legumin-like protein structures and foaming properties

2.3.1. Protein structure characterization

Native electrophoresis and SDS-PAGE under reducing conditions were used to identify legumin-like protein and measure its molecular weight with an AmershamTM ECLTM Gel Box (GE Healthcare Bio-Sciences Corp., Pittsburgh, PA, USA) using precast gel (4–20% gradient) and a constant voltage of 120 V. The weight-average molecular weight (M_w) of the legumin-like protein was determined by Size-Exclusion High-performance liquid chromatography (SE-HPLC) (Agilent series 1100, Palo Alto, CA, USA) equipped with a Zenix-C SEC-300 size exclusion column (3 μm, 300 A, 7.8 × 300 mm; Sepax Technologies, Inc., Newark, NJ, USA) at 22 °C. The flow rate was 0.5 mL/min and the elution was monitored at 280 nm.

The electrophoretic mobility of the extracted legumin-like protein samples under pH 2.0–11.0 at 22 °C was measured using a Zetasizer NanoS (model ZEN1600, Malvern Instruments Ltd., Malvern, UK). The hydrodynamic size of the legumin-like protein was determined by dynamic light scattering (DLS) using the same Zetasizer Nano ZS particle size analyzer with a backscatter detection angle of 173°.

Solubility was evaluated as reported previously [10] and expressed as the percentage of the protein in the supernatant compared to the total protein in the extract added into the suspension. The solubility profile was obtained by plotting the average protein solubility (%) against pH values.

Fluorescence intensity (FI) was determined for five concentrations of lentil legumin-like protein (0.0002–0.0010%) and ANS was used as the fluorescence probe. The excitation/emission wavelengths were set at 390 nm and 470 nm, respectively. Net FI of each solution (FI_{Net}) was calculated as: $(FI_{Net}) = (FI \text{ of protein dilution blank} - FI \text{ of protein solution with ANS})$. The initial slope of FI_{Net} versus protein concentration (% w/v) plot was calculated by linear regression analysis and used as an index (S_0) of the protein surface hydrophobicity.

The infrared spectra were recorded at 22 °C using a Nicolet 6700 spectrometer (Thermo Scientific, Madison, WI, USA) and Fourier self-deconvolutions were performed (FTIR) using the software provided with the spectrometer to study the amide I region of the protein. Band narrowing was achieved with a full width at half maximum of 15 cm⁻¹ and with a resolution enhancement factor of 2.5 cm⁻¹.

2.3.2. Foam morphology

Micrographs of the foam samples were observed with a Hitachi X-650 scanning electron microscope (SEM, Hitachi, Japan) at an acceleration voltage of 6 kV. Foams were frozen in liquid nitrogen immediately after prepared and freeze-dried. Then they were sputtered with gold for 2 min before SEM observation.

2.3.3. Foaming properties

Protein extract samples (1 g/100 mL) were dispersed in 30 mL of deionized water adjusted to pH 3.0, 5.0, or 7.0 using either 0.5 mol/L NaOH or 0.5 mol/L HCl solutions. The solution was mixed with a homogenizer (PowerGen 1000, Fisher Scientific, Fairlawn, NJ, USA). The foaming capacity (FC) was calculated as: $FC = (V_{f1} - V_{f0})/V_{f0} \times 100\%$, where V_{f0} and V_{f1} represent the volume of the protein solution and the formed foams after homogenization,

respectively. As an index of foam stability (FS), a “mean life” τ value was determined according to Eqs. (1)–(3) [11]. The larger the τ value, the longer the foam will last,

$$H(t) = H(0)\exp(-\lambda t) \quad (1)$$

where $H(0)$ is the initial foam height at time $t=0$, $H(t)$ is the foam height at time t , and λ is the decay constant, which is a measure of foam decay. This exponential relationship can be converted to a linear equation by taking the natural logarithm of the foam height, $\ln(H(t))$, vs time, where the slope value corresponds to $-\lambda$. τ is the inverse of the decay constant of a foam system.

$$\ln[H(t)] = \ln[H(0)] - \lambda t \quad (2)$$

$$\frac{d[\ln(H)]}{dt} = -\lambda = \frac{1}{\tau} \quad (3)$$

2.3.4. Surface properties

2.3.4.1. Shear rheology measurement. Surface phenomena are dependent on the bulk protein concentration [12], thus protein solutions of three different concentrations (10, 1 and 0.1 mg/mL) were prepared at pH 3.0, 5.0, and 7.0. Interfacial rheology of protein solutions at air–water interface were measured by means of a DHR3 rheometer (AT Instruments-Waters LLC, New Castle, DE, USA) using a Platinum/Iridium Du Noüy ring geometry (10 mm diameter). Strain sweep tests with strain amplitudes ranging from 0.01% to 100% were performed at 0.6283 rad/s in order to establish the linear viscoelasticity range. Then frequency sweep measurements (0.1–100 rad/s) were carried out at a strain amplitude of 0.1%; a value smaller than the critical value for linear viscoelasticity. The storage modulus G' and loss modulus G'' were recorded as a function of time during time sweep tests for up to 6.5 h at an oscillation frequency of 1 Hz and strain of 0.1%. The temperature of all the interfacial rheology tests was fixed at 22 °C.

2.3.4.2. Surface tension and dilatational rheology measurements. The surface tension of protein solutions was measured by the pendant drop technique with an automatic drop tensiometer (Model 400, Ramé-Hart Instrument Co., Succasunna, NJ, USA) at 22 °C [13]. The drop profile was fitted to the Young-Laplace capillarity equation to obtain the surface tension (γ). The dilatational rheological properties were measured with the same tensiometer at 22 °C using an oscillation with volume amplitude of 5% at a frequency of 0.1 Hz [14]. The measured change in surface tension during a surface area change over a sequence of four sinuses was used to determine the dilatational modulus. Each sample was measured at 22 °C in duplicate. The DROPIimage Advanced software (Ramé-Hart Inc., Mountain Lakes, NJ, USA) was used for data collection and analysis. The surface dilatational modulus, E , is defined in Eq. (4) and is the change in surface tension (γ) upon a small change in surface area (A) of a constant shape [15], and the surface dilatational elastic and loss moduli E' and E'' are correlated with the dilatational modulus E of the interface by Eq. (5).

$$E = \frac{d\gamma}{(dA/A)} = \frac{d\pi}{\ln A} \quad (4)$$

$$E = \left(\frac{\gamma_0}{A_0} \right) (\cos \phi + i \sin \phi) = E' + iE'' \quad (5)$$

where, π is the surface pressure, γ_0 and A_0 are the strain and stress amplitudes, respectively, and ϕ is the phase angle between stress and strain. The ratio (γ_0/A_0) is the absolute modulus $|E|$, a measure of dilatational resistance to deformation [15].

2.4. Statistics analysis

All samples were tested in triplicate and results are presented as mean \pm SD. One way or two way analysis of variance (ANOVA)

was carried out using Origin 9.1 software (Origin Lab Corporation, Northampton, MA, USA), and statistical differences among sample means were determined using Tukey's test at 95% confidence level.

3. Results and discussion

3.1. Lentil legumin-like protein structures

Rate-zonal centrifugation of lentil legumin-like protein resulted in a sedimental velocity of 13S. Native electrophoresis result (Fig. 1A, lane N) shows a band with a molecular weight between 346 and 426 kDa. Typically, legumin hexamers consist of six subunits of approximately 60 kDa that interact non-covalently, each one comprised of an acidic subunit (α) of around 40 kDa and a basic subunit (β) of approximately 20 kDa, linked by a single disulfide bond. SDS-PAGE of lentil legumin-like protein under reducing conditions (Fig. 1A, lane F) shows three bands with relative molecular weights of 32, 42, and 47 kDa, respectively, corresponding to the acidic polypeptide chains. The other two bands at 18 and 20 kDa correspond to the two basic polypeptide chains. Similar legumin subunits were previously identified in lentils [4], peas, soybeans and fava beans [16]. Previous study done by Aydemir and Yemencioğlu [8] in crude lentil protein and protein extract identified bands between 15 and 20 kDa, 30 and 40 kDa, and 40 and 70 kDa for the crude protein using SDS-PAGE, while for isoelectric precipitated extract they found intensive spots of protein between 21–23 kDa and around 26 kDa, and less intense spots above 30 kDa [8]. The protein bands identified in this work for lentil legumin-like protein are more similar to the crude protein extract of Aydemir and Yemencioğlu work. Fig. 1B shows the SE-HPLC chromatogram of the lentil legumin-like protein. The sample possesses one major peak with a weight-average molecular weight of 347 kDa. This result is in good agreement with that observed in the SDS-PAGE

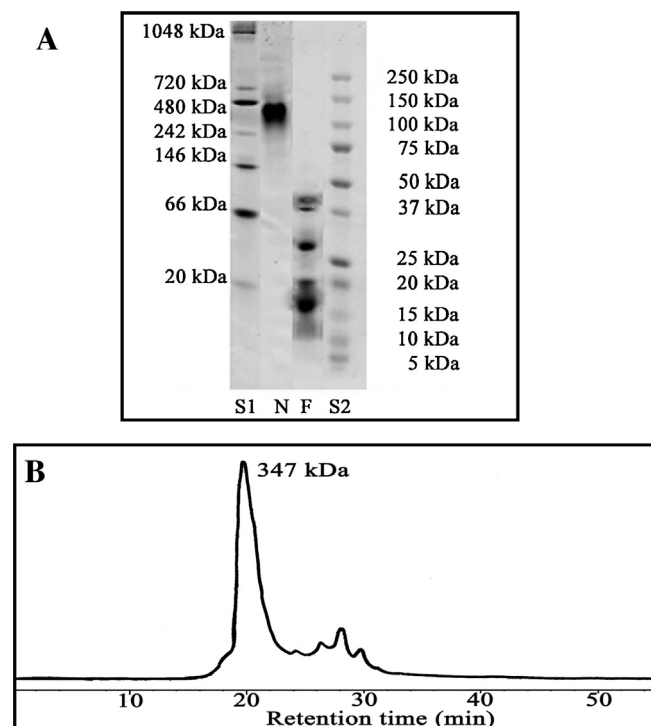


Fig. 1. (A) Lentil legumin-like protein under (N) native gel and (F) SDS-PAGE gel conditions. S1 and S2 are protein molecular standards in native and SDS-PAGE gel, respectively. (B) SE-HPLC chromatogram of lentil legumin-like globulin enriched fraction.

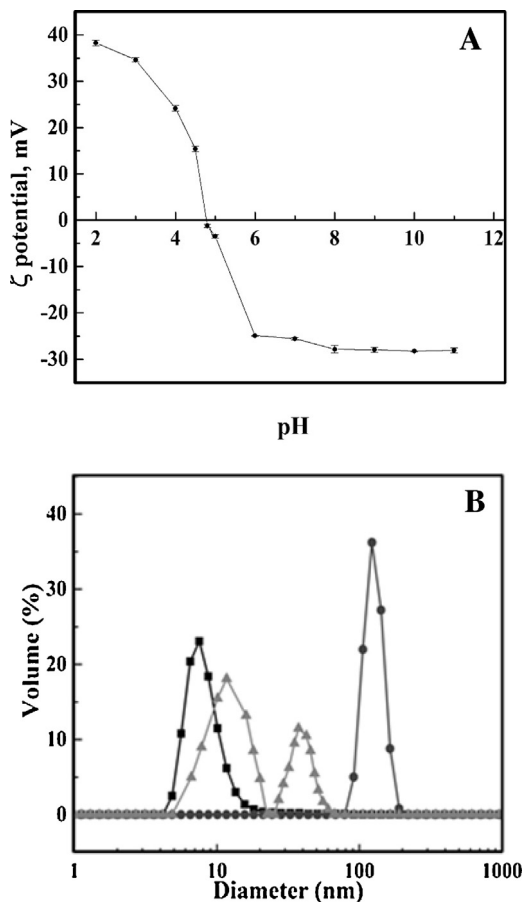


Fig. 2. (A) ζ -Potential of lentil legumin-like protein as a function of pH. Values are reported as mean \pm standard deviation. (B) Molecular size of lentil legumin-like protein in solution at pH 3.0 (square), pH 5.0 (circle), and pH 7.0 (triangle).

pattern. Small peaks appearing in the chromatogram might be identified as small amounts of 7S and 3S proteins present in the sample [17].

The amino acid composition analysis (methodology and results provided in Table S1, supplementary data) revealed that similar to most legume globulin proteins, lentil legumin-like protein is rich in glutamine/glutamic acid, asparagine/aspartic acid (about 26% in total) and glycine (9%), but poor in sulfur containing amino acids (1%), methionine and cysteine. This protein exhibited balanced hydrophilic and hydrophobic segments with ~40% hydrophobic residues including alanine, valine, isoleucine, leucine, phenylalanine and proline, and ~38% hydrophilic residues including glutamine/glutamic acid, asparagine/aspartic acid, lysine and arginine.

As shown in Fig. 2A, lentil legumin-like protein has an isoelectric point (pI) around 4.6. The highest charge reached +38 mV at pH 2.0 and -28 mV at alkaline pH from 8.0 to 11.0. The hydrodynamic size distribution of lentil legumin protein at different pH is shown in Fig. 2B. The protein sample presented monomodal size distributions at both pH values: 3.0 and 5.0, with a peak at 7 nm and 120 nm, respectively. While a bimodal distribution with two peaks at 12 and 40 nm was observed at pH 7.0. According to Ruiz-Henestrosa et al. [18], estimated size of glycinin assembled forms 3S and 11S are 6.8 and 14.6 nm, respectively. Dissociation of the 13S into 7S or 3S was observed in pea legumin, soy glycinin, and lupin legumin [19]. Thus, the hydrodynamic size observation suggests that lentil legumin-like protein was dissociated from 13S into 3S form at pH 3.0. At pH 5.0, the charge of lentil legumin-like protein is close to 0 because of

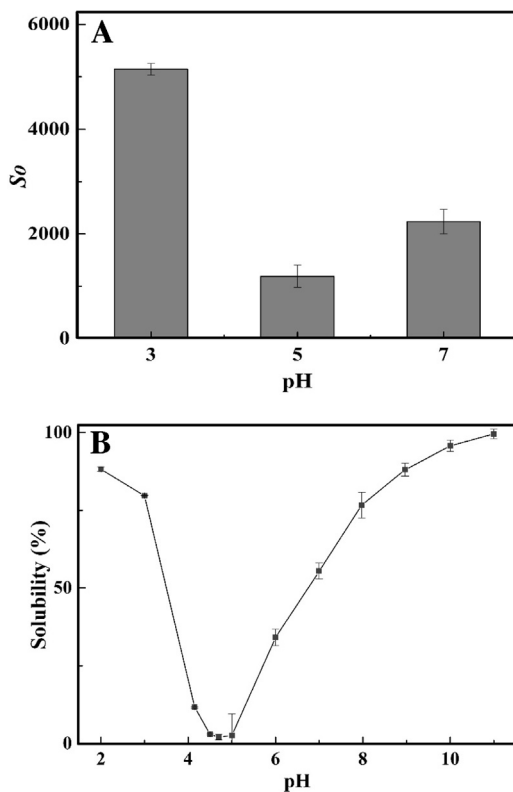


Fig. 3. (A) Surface hydrophobicity index (S_0) and (B) solubility of lentil legumin-like protein as a function of pH. Values are reported as mean \pm standard deviation.

the proximity to its isoelectric point. In the presence of minimum electrostatic repulsion, protein aggregation could occur, leading to increased size. At pH 7.0, the major peak represents 13S protein while the smaller peak represents small aggregates. The presence of some aggregates at pH 7.0, but not at pH 3.0 may be related to the lower net surface charge (-25 mV compared to +35 mV). These small aggregates might not be detected during SE-HPLC analysis due to M_w exclusion limit of the column and the presence of a guard column.

As shown in Fig. 3A, the surface hydrophobicity was the lowest at pH 5.0 (S_0 value of 1200), but dramatically increased at pH 3.0 and 7.0 with S_0 values of 5200 and 2200, respectively. The S_0 values determined by ANS are, higher than those reported for other legumins such as pea and soybean, which had S_0 values from 94 to 2000 [20]. Higher surface hydrophobicity of lentil legumin-like protein might be attributed to a higher exposure of aromatic and aliphatic amino acid residues. Lower S_0 values were observed at pH 5.0 because protein tended to aggregate when pH was near its pI, thus hydrophobic groups become hidden inside the aggregates and less accessible to ANS. Higher S_0 value observed at pH 3.0 than 7.0 can be related to dissociation of legumin-like proteins at pH 3.0 to expose more hydrophobic regions [21]. In addition, ANS as an anionic probe could interact with positively charged sites on the proteins at low pH, thus resulting in overestimation of hydrophobicity to a certain extent [22].

Lentil legumin-like protein showed minimum solubility around 4.7 (near pI), with protein solubility increasing dramatically when pH deviated from the pI. Relatively high solubility was observed at pH 2 (above 85%) and above pH 8 (70–95%) (Fig. 3B), which is favorable for its potential applications. It is interesting to notice that lentil legumin-like protein possesses both high surface hydrophobicity and solubility when pH was deviated from protein pI, thus it

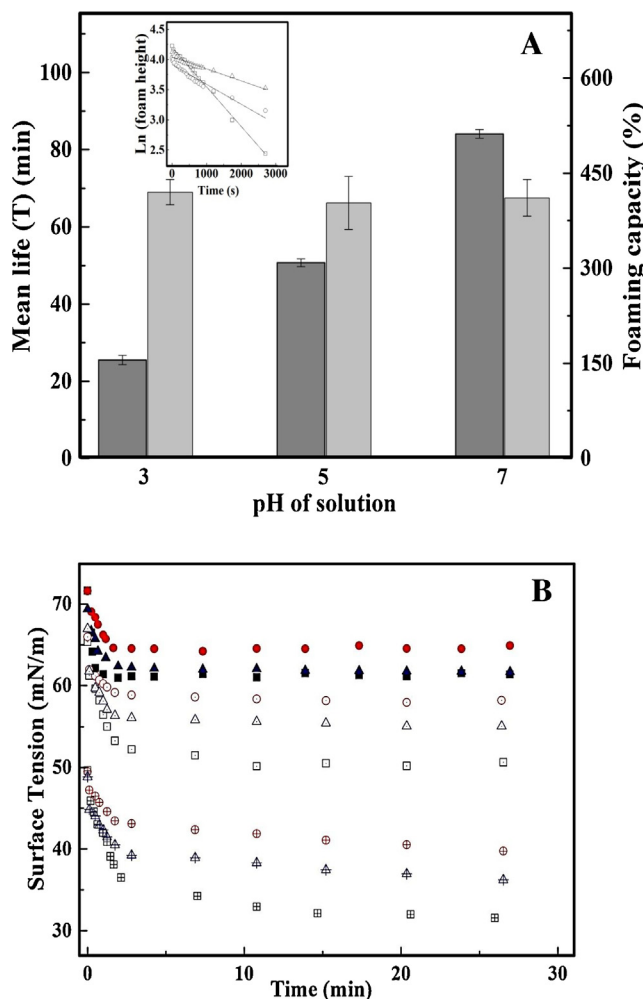


Fig. 4. (A) Mean life (dark gray bars) and foaming capacity (light gray bars) values of foams stabilized by lentil legumin-like protein at pH 3.0, 5.0, and 7.0. The insert shows the plot of natural logarithm of foam height at pH 3.0 (squares), 5.0 (circles), and 7.0 (triangles) versus time which was used to calculate mean life. The fitting of the models (R^2) was higher than 0.92 in all cases. (B) Surface tension of lentil legumin-like protein versus time in solutions at pH 3.0 (square), pH 5.0 (circle), and pH 7.0 (triangle) (solid symbol: 0.1 mg/mL, open symbol: 1 mg/mL, crossed symbol: 10 mg/mL). Values are reported as mean \pm standard deviation.

is likely that a balanced level of hydrophilic and hydrophobic amino acid residues are exposed at the protein surface.

3.2. Foaming properties

The foaming capacity (FC) as a function of pH is presented in Fig. 4A. The FC is high at all pH levels, ranging from 403 to 425%, which is better than that reported for soy and pea 11S protein at similar pH range [13]. Fig. 4A insert shows the fitting of the experimental data of natural logarithm of foam height versus time for the lentil legumin-like protein. From these plots, the mean lifetime (τ) was calculated giving values of 25.5, 50.7, and 84.1 min for pH 3.0, 5.0, and 7.0, respectively (Fig. 4A). A foam can decay smoothly or collapse very fast. Foams formed at pH 5.0 and 7.0, which is the common pH range for most food and non-food applications, can be classified as long life foams which normally show decay τ value of 50 min or higher [23]. Long life foams are particularly useful in the food industry when products must be processed for long periods and it is important to keep the aerated structure before solidifying or gelling (e.g. mousse and ice cream).

3.3. Impact of protein structure on surface properties

The good foaming properties of lentil legumin-like protein observed above drove us to investigate how protein molecular structure influences surface phenomena and the subsequent foaming properties.

3.3.1. Surface tension

Reducing surface tension involves proteins migrating to the air-water interface and forming a layer or film by adsorbing and re-orienting themselves. Increasing the bulk concentration until a certain concentration of protein will speed the decay of surface tension because of the higher number of molecules that transport and adsorb to the interface [24]. The decrease in the surface tension with increasing concentration of protein was also observed by Tomczynska-Mleko et al. [25] in whey protein isolate. At higher values (6–11%) the whey protein concentration does not affect the change in the surface tension, likely due to a complete coverage of the surface by proteins at that point [25]. This is also observed in lentil legumin-like protein, as shown in Fig. S1 (supplementary data). Critical micelle concentration (cmc) of our protein is 5 mg/mL, from where no further decrease is observed in static surface tension.

In addition, the rate of surface tension decay will increase because of increased diffusion and adsorption of the molecules. As diffusion is inversely proportional to the cube root of the molecular weight, smaller molecules will move and adsorb faster to the interface compared to the larger molecules [15]. In addition, proteins with a flexible structure and higher surface hydrophobicity possess more capacity of lowering surface tension because they can strongly adsorb at the interface [26]. As shown in Fig. 4B, higher protein concentration led to lower values of surface tension. The capacity for lentil legumin-like protein to reduce surface tension follows the sequence of pH 3.0 > pH 7.0 > pH 5.0. This correlates well with previously characterized protein structures at different pH. Lentil legumin-like protein showed smaller size, higher solubility and surface hydrophobicity at pH 3.0 than pH 7.0 thus could migrate and adsorb onto the water/air interface more rapidly at acidic pH than at neutral pH. On the other hand, large size, low solubility, and surface hydrophobicity at pH 5.0 resulted in a relatively low surface activity. Lentil legumin-like protein showed a similar capacity for decreasing the surface tension when compared to β -lactoglobulin and soy glycinin at pH 7.0 [13]. Study of pH influence on surface tension of whey protein isolate by Tomczynska-Mleko et al. [25], it also showed a better capacity of reducing surface tension at pH 3.0 than at other pH values, but a lower surface activity at pH 7.0 than lentil legumin-like protein. Since surface tension is not only related to electric charge of the protein but also to other physic-chemical characteristics of the protein, differences between whey protein and lentil legumin-like protein are likely related to the latter.

3.3.2. Surface rheology

Surface shear rheological parameters are sensitive to surface composition and protein-protein interactions [27], and normally higher values of storage modulus (G') indicate stronger interactions. As shown in Fig. 5A, higher protein concentration led to higher G' values ($p < 0.05$) due to more intermolecular interactions and strengthening of non-covalent bonds within adsorbed layer of proteins [27,28]. During the whole test period G' was 10 fold higher than G'' (data for G'' not shown). This result indicates that legumin-like lentil protein was able to form an elastic network at the water/air interface at all the pH level tested, which plays an important role contributing to the foam stability as an elastic film and can better resist deformation and also recover its natural shape when the deforming force is removed. The G' value increased more

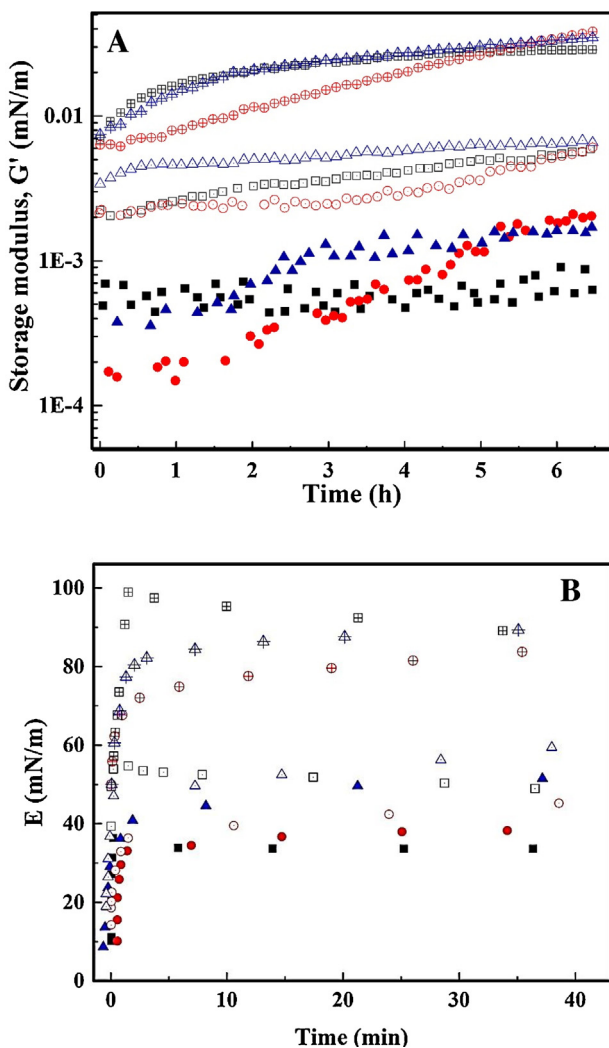


Fig. 5. (A) Shear storage modulus (G') and (B) dilatational modulus (E) of lentil legumin-like protein versus time in solutions at pH 3.0 (square), pH 5.0 (circle), and pH 7.0 (triangle) (solid symbol: 0.1 mg/mL; open symbol: 1 mg/mL; crossed symbol: 10 mg/mL).

rapidly at pH 3.0 and 7.0 especially at 10 mg/mL due to the fast protein diffusion and adsorption because of the higher solubility and smaller hydrodynamic diameter. In addition, their higher surface hydrophobicity could facilitate protein adsorption at the air/water interface. A different kinetic of adsorption was observed at pH 5.0, where lag times (initial time where no change in the surface properties was observed) were indicative of slower diffusion of the protein

molecules to the interface and hindered adsorption due to the low molecules flexibility and susceptibility to conformational changes due to aggregation [13]. It is noticed that the G' values at pH 5 still showed increasing trend even after 6 h at all the pH level tested. This is generally related to protein multilayer building at the interface, which might in part explain the high stability of the foam [29]. The end values of G' were higher at pH 5.0 and 7.0 at the protein concentrations of 10 and 0.1 mg/mL and similar at different pHs when concentration was 1.0 mg/mL.

The evolution of the surface dilatational modulus (E) with time is shown in Fig. 5B. E value is the result of the intra-protein flexibility and the aggregated inter-protein network strength [30]. It is also correlated with diffusion and adsorption of protein molecules toward the interface [15]. At pH 3.0 a faster network building generated higher values of elasticity at a short time (<2 min) due to higher protein diffusion. Though the dilatational elasticity of the surface layer at pH 7.0 and 5.0 did not reach the same level as that at pH 3.0 at the initial stage, they became similar in the relatively long time period (>10 min). The decayed E value suggests that less strong elastic protein networks could be maintained at the air-water interface at pH 3.0.

3.3.3. Kinetic study

At surface pressure values where diffusion process is the rate-determining step of protein adsorption at the interface, a modified form of the Ward and Torday equation can be used to calculate the diffusion coefficient [13]:

$$\pi = 2C_0KT \left(\frac{k_{diff} t}{3.14} \right)^{1/2} \quad (7)$$

where π is the surface pressure calculated as the change in surface tension compared to water value, C_0 is the protein concentration in solution, k_{diff} is the diffusion coefficient, K is the Boltzmann constant, T is the absolute temperature, and t is the time. Then, a plot of π vs $t^{1/2}$ should be linear with a slope equal to the diffusion coefficient. The plots for all the samples gave a straight line at the initial stage (data not shown). As shown in Table 1, k_{diff} is higher at higher protein concentration in the bulk phase and the value for k_{diff} decreases in the sequence pH 3.0 > pH 7.0 > pH 5.0 as k_{diff} increases as the hydrodynamic size decreases according to the Stokes-Einstein equation.

After diffusion control step, the protein adsorption kinetic can be evaluated using the first-order rate equation [13,15]:

$$\ln \left[\frac{\pi_\infty - \pi_t}{\pi_\infty - \pi_0} \right] = -kt \quad (8)$$

where π_∞ , π_t , and π_0 are the surface pressures at the steady or equilibrium state, at any time t , and at $t=0$, respectively, and k is the first-order rate constant. The plot of $\ln [(\pi_\infty - \pi_t)/(\pi_\infty - \pi_0)]$

Table 1

Characteristic interfacial parameters for the diffusion, adsorption, and rearrangement at the air–water interface.

pH	Concentration (mg/mL)	k_{diff} (mN m ⁻¹ s ^{-0.5}) ^A	k_{ads} ($\times 10^{-5}$ s ⁻¹) ^A	k_{reag} ($\times 10^{-5}$ s ⁻¹) ^A
3	0.1	0.12 ± 0.01 ^{a,x}	2.01 ± 0.6 ^{a,x}	8.16 ± 0.8 ^{a,x}
5	0.1	0.07 ± 0.02 ^{a,y}	1.06 ± 0.1 ^{a,y}	10.4 ± 0.5 ^{a,y}
7	0.1	0.09 ± 0.04 ^{a,z}	1.99 ± 0.5 ^{a,x}	12.3 ± 0.7 ^{a,y}
3	1.0	0.24 ± 0.02 ^{b,x}	2.80 ± 0.2 ^{b,x}	9.62 ± 0.3 ^{b,x}
5	1.0	0.20 ± 0.03 ^{b,y}	2.23 ± 0.3 ^{b,y}	15.9 ± 0.2 ^{b,y}
7	1.0	0.21 ± 0.06 ^{b,z}	3.01 ± 0.3 ^{b,x}	18.8 ± 0.1 ^{b,y}
3	10	0.26 ± 0.02 ^{c,x}	2.94 ± 0.1 ^{b,x}	17.7 ± 0.6 ^{c,x}
5	10	0.21 ± 0.05 ^{c,y}	2.45 ± 0.1 ^{b,y}	21.6 ± 0.3 ^{c,y}
7	10	0.24 ± 0.06 ^{c,z}	3.19 ± 0.2 ^{b,x}	27.3 ± 0.9 ^{c,y}

Linear regression coefficient are all higher than 0.91.

^A Values are presented as mean ± SD.

(a,b,c) Significant differences among samples due to concentration ($p < 0.05$).

(x,y,z) Significant differences among samples due to pH ($p < 0.05$).

versus θ is characterized by two regions: the first one corresponding to the adsorption period (or penetration of the interface), and the second one for the rearrangement period, each one characterized by its own constant, k_{adsp} and k_{reag} [15]. Adsorption is favored by exposition of hydrophobic residues [31], so that protein molecules with higher surface hydrophobicity, as at pH 3.0 and 7.0 (Fig. 3A) exhibited higher adsorption rate (k_{adsp}). Smaller protein size (less aggregates) also contributed to protein adsorption at the interface. After the protein has been adsorbed, the rearrangement process takes precedence. According to Beverung et al. [32], in the rearrangement process, proteins continue to slowly change their conformation and build a viscoelastic interfacial film. Additional layers might be added in the monolayer interface when conformational changes of adsorbed proteins provide a favorable environment for sublayer proteins to interact with the adsorbed molecules. As shown in Table 1, high k_{reag} values at pH 7.0 and pH 5.0 were observed compared to those at pH 3.0. Considering the fact that long life foams were obtained at 7.0 and 5.0 (Fig. 4A), the rearrangement process is likely to play a major role contributing to the formation of a stronger surface network, leading to improved foam stability. In order to have a better understanding of this system, protein molecules rearrangement at the interface was investigated using FTIR in the next step.

3.4. FTIR spectra of protein in solution and at the foam surface

Fig. 6A shows the FTIR spectra in the amide I region of the legumin-like protein prepared at pH 3.0, 5.0, and 7.0. Beta-sheet (1632 cm^{-1}) and β -turn (1660 cm^{-1}) structures are the major secondary structures for lentil legumin-like protein at all pH tested. This is typical for most of legumins, which indicates that about two-thirds of the amino acid residues in each of the subunits are involved in β -sheet and turn conformations [2]. The fact that lentil legumin-like protein is rich in Asp, Asn, and Gly (Table S1, supplementary data) might explain these structures, since the presence of a glycine residue close to the Asn/Asp residue provides additional flexibility in the main chain that enables the turn structures [33]. Beta-structures can be amphipathic with alternating hydrophobic and hydrophilic residues, which creates a hydrophobic and a hydrophilic segment [33]. Even when most of hydrophobic residues might be buried in the core of the globular protein, some bulky ones, such as phenylalanine and tyrosine, could stay on the surface, creating hydrophobic patches and increasing the surface hydrophobicity of the molecule [34]. When pH changed to 7.0 and 3.0, the portion of β -sheets ($1628\text{--}1632\text{ cm}^{-1}$) decreased to a certain extent, probably induced by charge change on protein molecular chains.

FTIR was also applied to study protein conformational changes when adsorbed at the interface and the spectra are shown in Fig. 6B. Compared to the lentil legumin-like protein solutions, a major peak at around 1651 cm^{-1} that corresponds to α -helix can be identified at pH 7.0, along with β -sheets ($1634\text{ and }1683\text{ cm}^{-1}$) and β -turns (1670 cm^{-1}). The absorption at 1618 cm^{-1} suggests formation of protein aggregates at the interface. At pH 5.0, a strong aggregation is observed (1620 cm^{-1}), as well as β -sheets (1634 cm^{-1}) and β -turns ($1663\text{ and }1677\text{ cm}^{-1}$). At pH 3.0, the adsorbed protein is characterized by unordered structure (1642 cm^{-1}), β -turns (1661 and 1677 cm^{-1}), and some aggregates (1624 cm^{-1}).

Based on these spectra, it is suggested that lentil legumin-like protein conformation changed when adsorbed at the interface, depending on environmental pH. At pH 7.0, lentil legumin-like protein formed α -helix structure at the interface. The presence of α -helix structure could contribute to formation of more stable interfaces and multilayer interfaces, likely due to possible creation of more non-covalent intramolecular interactions. Alpha-Helices could be adsorbed with their long axis parallel to the

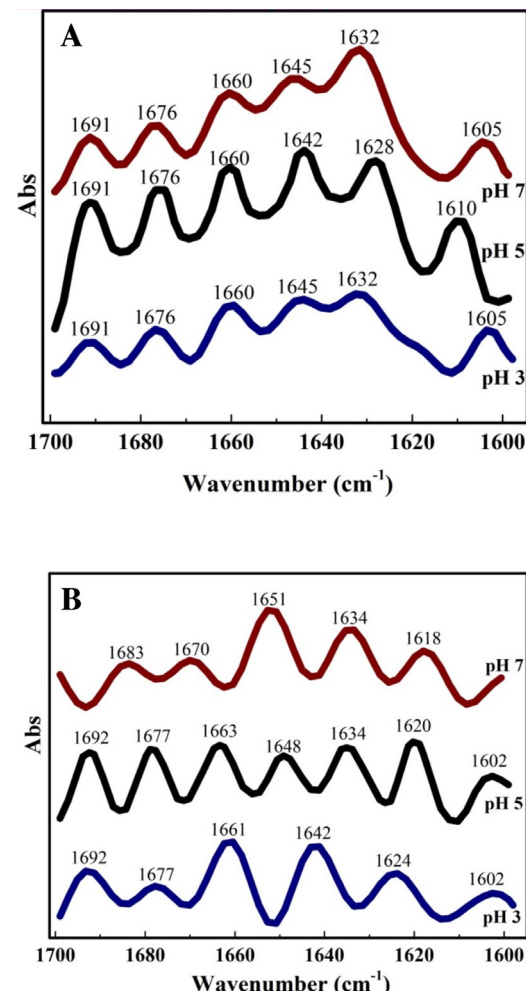


Fig. 6. Fourier-deconvoluted FTIR spectra of lentil legumin-like protein in (A) solution and (B) at the foam surface at pH 3.0, 5.0, and 7.0.

air/liquid interface, which would allow the side chains that protrude to interdigitate, so α -helices would be packaged side by side [35]. At pH 5.0, the slower protein adsorption rate together with the minimum electrostatic repulsion allowed lentil legumin-like protein to build a strong aggregated multilayer interface that helped foam to resist collapse. The presence of β -structures could contribute to strong interfacial network building because of its rigidity [36]. These molecular structures could partially explain the high stability of lentil legumin-like protein stabilized foams at pH 5.0 and 7.0 (Fig. 4A). Whereas at pH 3.0 unstructured structures increased intra-protein flexibility, producing a less compact structure and relaxed interface that reduces elasticity modulus [30]. Consequently, the foam would have a lower resistance against collapse.

Tomczynska-Mleko et al. [25] studied the effect of pH on the structure of whey protein isolate in relation to its surface activity and observed that partial unfolding of proteins associated with a reduction in the number of α -helix structures and an increasing number of disordered structures, causes a decrease in the surface tension of the protein solutions, likely due to a more flexible protein structure that can increase the adsorption at the interface.

3.5. Foam morphology

Scanning electron microscopy (SEM) observation of foam at pH 3.0 showed a less compact structure (insert of Fig. 7A) and

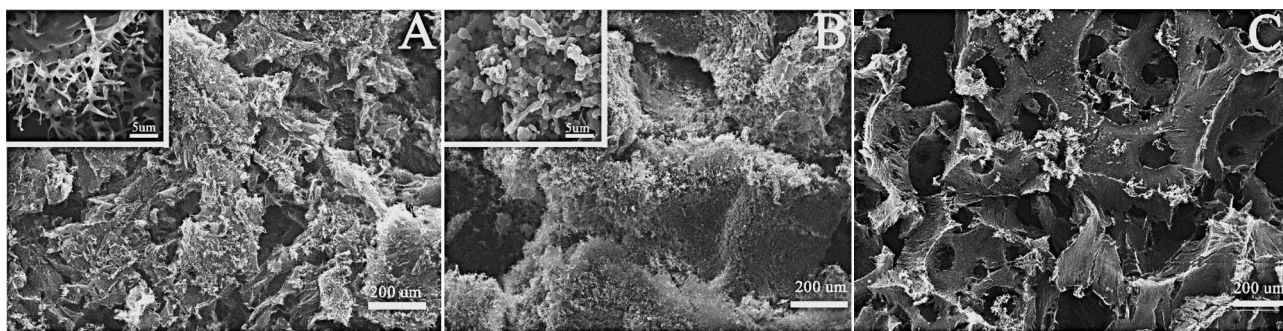


Fig. 7. SEM micrographs of foams produced from lentil legumin-like protein at (A) pH 3.0, (B) pH 5.0, and (C) pH 7.0.

it seems the overall foam structure collapsed after freeze drying. Foam morphology at pH 5.0 (insert of Fig. 7B) exhibits a particulate morphology characteristic of protein networks formed at pH near its pl. Such network is composed of randomly aggregated protein particles forming a thick and dense interface film. The foam prepared at pH 7.0 shows a dense and almost homogeneous network where holes left by bubbles are clearly visible (Fig. 7C), suggesting strong interfacial networks were formed which could well maintain shape and structure during the freeze-drying process.

4. Conclusions

This research revealed the high foaming capacity of lentil legumin-like protein and long life foams were obtained at pH 5.0 and 7.0. Studies of the foaming kinetics and protein conformation suggest that the foaming stability of lentil legumin-like protein was dependent on conformation of the protein at the air-water interface that strongly affected adsorption and re-organization of the protein layer at the interface. Foams prepared at pH 7.0 showed dense and strong networks at the interface, where combination of the α -helix secondary structure, medium hydrodynamic molecular size, and balance between solubility/hydrophobicity all contributed to building of strong protein networks at the interface. At pH 5.0, the protein formed dense and thick interface network composed of randomly aggregated protein particles. At pH 3.0, the smaller hydrodynamic size and high surface hydrophobicity led to formation of an initially elastic surface layer. However, the unordered structure increased intra-protein flexibility producing a less compact structure and relaxed interface that reduces elasticity modulus with time. Consequently, the foam would have a lower resistance against collapse. This research also provides support information for potential use of lentil protein as a foaming ingredient in food and non-food products where long life foams are required.

Acknowledgments

The authors are grateful to the Natural Sciences and Engineering Research Council of Canada (NSERC), Alberta Crop Industry Development Fund Ltd. (ACIDF) and Alberta Innovates Bio Solutions (AI Bio) for financial support as well as Canada Foundation for Innovation (CFI) for equipment support. Lingyun Chen thanks the Natural Sciences and Engineering Research Council of Canada (NSERC)-Canada Research Chairs Program for its financial support. Marcela Jarpa thanks CONICYT-Chile for the support given through the scholarship Becas Chile.

Appendix A. Supplementary data

Supplementary material related to this article can be found, in the online version, at <http://dx.doi.org/10.1016/j.colsurfb.2015.04.065>.

References

- [1] M.T. Nickerson, J.D. House, E.C. Li-Chan, 08 July 2013 [Online]. Available: <http://canadianfoodinsights.com/2013/07/08/canadian-proteins/> (accessed 22.09.14).
- [2] P. Argos, S. Narayanan, N.C. Nielsen, *EMBO J.* 4 (5) (1985) 1111–1117.
- [3] Statistics Canada and Industry Consultations, 11 November 2014 [Online]. Available: <http://www.agr.gc.ca/eng/industry-markets-and-trade/statistics-and-market-information/by-> (accessed 18.12.14).
- [4] C. Barbana, J.I. Boye, *Food Chem.* 127 (2011) 94–101.
- [5] P.R. Shewry, R. Casey, *Seed Proteins*, Springer Science + Business Media B.V., Dordrecht, 1999.
- [6] P. Chakraborty, F. Sosulski, A. Bose, *J. Sci. Food Agric.* 30 (1979) 766–771.
- [7] R. Toews, N. Wang, *Food Res. Int.* 52 (2013) 445–451.
- [8] L.Y. Aydemir, A. Yemencioğlu, *LWT – Food Sci. Technol.* 50 (2013) 686–694.
- [9] M. Jarpa-Parra, F. Bamdad, Y. Wang, Z. Tian, F. Temelli, J. Han, L. Chen, *LWT – Food Sci. Technol.* 57 (2014) 461–469.
- [10] S. Abe, E. Davies, *Memoirs of the College of Agriculture*, vol. 31, Ehime University, 1986, pp. 187–199.
- [11] J.J. Hackbarth, *J. Inst. Brew. Distilling* 112 (1) (2006) 17–24.
- [12] J. Rodríguez-Patino, S. Molina-Ortiz, C. Carrera-Sánchez, M. Rodríguez-Niño, M. Añón, *J. Colloid Interface Sci.* 268 (2003) 50–57.
- [13] V. Ruiz-Henestrosa, C. Carrera-Sánchez, M. Yust-Escobar, J.J. Pedroche-Jimenez, F. Milla-Rodríguez, J.M. Rodriguez-Patino, *Colloids Surf. A: Physicochem. Eng. Aspects* 309 (2007) 202–215.
- [14] J. Davis, E. Foegeding, *J. Food Sci.: Food Chem. Toxicol.* 69 (5) (2004) C404–C410.
- [15] J.M. Rodriguez-Patino, M.R. Rodriguez-Niño, C. Carrera-Sánchez, S.E. Molina-Ortiz, M.C. Añón, *J. Food Eng.* 68 (2005) 429–437.
- [16] A. Kimura, T. Fukuda, M. Zhang, M.S.N. Maruyama, S. Utsumi, *J. Agric. Food Chem.* 56 (2008) 10273–10279.
- [17] B. Oomah, H. Voldeng, J. Fregeau-Reid, *Plant Foods Hum. Nutr.* 45 (1994) 251–263.
- [18] V. Ruiz-Henestrosa, M. Martinez, J. Patino, A. Pilosof, *J. Am. Oil Chem. Soc.* 89 (2012) 1183–1191.
- [19] J. Gueguen, M. Chevalier, J. Barbot, F. Schaeffer, *J. Sci. Food Agric.* 44 (1988) 167–182.
- [20] A. Karaca, N. Low, M. Nickerson, *Food Res. Int.* 44 (2011) 2742–2750.
- [21] J. Gueguen, P. Cerletti, *New and Developing Sources of Food Proteins*, Chapman & Hall, London, 1994, pp. 145–194.
- [22] N. Alizadeh-Pasdar, E.Y. Li-Chan, *J. Agric. Food Chem.* 48 (2000) 328–334.
- [23] L. Piazza, J. Gigli, A. Bulbarello, *J. Food Eng.* 84 (2008) 420–429.
- [24] L.K. Shrestha, Y. Matsumoto, K. Ihara, K. Aramaki, *J. Oleo Sci.* 9 (57) (2008) 485–494.
- [25] M. Tomczynska-Mleko, E. Kamysz, E. Sikorska, C. Puchalski, S. Mleko, L. Ozimek, G. Kowaluk, W. Gustaw, M. Wesolowska-Trojanowska, *Czech J. Food Sci.* 32 (1) (2014) 82–89.
- [26] E. Cases, C. Rampini, P. Cayot, *J. Colloid Interface Sci.* 282 (2005) 133–141.
- [27] E. Dickinson, *Food Hydrocolloids* 25 (2011) 1966–1983.
- [28] S. Mleko, H. Kristinsson, Y. Liang, M. Davenport, W. Gustaw, M. Tomczynska-Mleko, *LWT – Food Sci. Technol.* 43 (2010) 1461–1466.
- [29] J. Benjamins, E. Lucassen-Reynder, *Interfacial rheology of adsorbed protein layers*, in: R.M., L. Liggieri (Eds.), *Interfacial Rheology*, CRC Press, Taylor & Francis Group, Boca Raton, FL, 2009, pp. 253–302.

- [30] L.G. Cascao-Pereira, O. Theodoly, H.W. Blanch, C.J. Radke, *Langmuir* 19 (2003) 2349–2356.
- [31] P. Wierenga, H. Gruppen, *Curr. Opin. Colloid Interface Sci.* 15 (2010) 365–373.
- [32] C. Beverung, C. Radke, H. Blanch, *Biophys. Chem.* 81 (1999) 59–80.
- [33] G.A. Petsko, D. Ringe, *Protein Structure and Function*, New Science Press Ltd., London, 2004, pp. 5–6.
- [34] F. Bamdad, J. Wu, L. Chen, *J. Cereal Sci.* 54 (1) (2011) 20–28.
- [35] P. Lavigne, P. Tancréde, F. Lamarche, J.-J. Max, *Langmuir* 8 (1992) 1988–1993.
- [36] A.H. Martin, M.B.J. Meinders, M.A. Bos, M.A. Cohen Stuart, T. van Vliet, *Langmuir* 19 (2003) 2922–2928.